J Physiol Sci (2015) 65 Suppl 2: S-29 – S-35

ORIGINAL PAPER

The estrous cycle modulates voltage-gated ion channels in trigeminal ganglion neurons

Wachirapong Saleeon · Ukkrit Jansri · Anan Srikiatkhachorn · Saknan Bongsebandhu-phubhakdi

Abstract Migraines typically occur more frequently in women than men because of the effects of estrogen on both the frequency and severity of migraine attacks. Many women suffer from migraine attacks during menstruation, which are known as menstrual migraines. The pathophysiology of menstrual migraines can be explored by using the rat estrous cycle, which shows a cyclical fluctuation of estrogen level that resembles the menstrual cycle. The aim of this study was to investigate whether different stages of the estrous cycle are involved in migraine development by comparing the excitability of trigeminal ganglion (TG) neurons in four different stages of the estrous cycle by using action potential (AP) parameter assessments. The stages of the estrous cycle were identified by a vaginal smear and measuring the estrogen levels in collected blood. The proestrus and estrus stages had higher estrogen levels compared with the diestrus and metestrus stages. Whole-cell patch clamp recordings demonstrated that TG neurons in the proestrus and estrus stage had lower AP threshold, lower rheobase, higher AP height, shorter AP falling time and deeper after-hyperpolarization (AHP) depth. Hence, our results revealed that the high level of estrogen in the proestrus and estrus stage alters the AP properties of TG neurons. Estrogen may increase membrane excitability and the summation of cellular responses, which alters the AP properties. The alterations of the AP properties in the proestrus and estrus stage may relate to a modification of voltage-gated ion channels in TG neurons, which is a pathogenesis for menstrual migraine. No COI.

W. Saleeon · S. Srikiatkhachorn
Department of Physiology, Faculty of Medicine, Chulalongkorn University, 1873 Rama IV Road, Pathumwan, Bangkok, Thailand

U. Jansri · S. Bongsebandhu-phubhakdi (✉)
Research Affairs, Faculty of Medicine, Chulalongkorn University, 1873 Rama IV Road, Pathumwan, Bangkok, Thailand
e-mail: saknan@live.jp

Keywords Menstrual migraine · Estrous cycle · Trigeminal ganglion (TG) neurons · Whole-cell patch clamp recording · Voltage-sensitive ion channels

Introduction

Migraine occurs more often in women than in men. More than 50% of women experience menstrual cycle-related migraine [1, 2]. The menstrual cycle enhances various parameters of a migraine, such as the severity, duration and frequency of painful migraine attacks. Previous research suggests that fluctuation of estrogen level during the menstrual cycle can affect menstrual migraine [3]. The incidence of migraine attacks peaks on the days before and after the onset of menstruation [4]. Estrogen levels fluctuate during each stage of the menstrual cycle, which is divided into follicular and luteal phases. In female rats, the menstrual cycle is called the estrous cycle and occurs in four stages, diestrus, proestrus, estrus and metestrus. Estrogen levels peak during proestrus and estrus. The duration of estrous cycle is very short compared with human menstrual cycle (4-5 days and 28 days, respectively). Hormonal fluctuation in estrous cycle of rat is quite similar to human menstrual cycle [5]. In both cycles, there were marked increases of estrogen level at the latter half of preovulatory phase followed by rapid decreases before the initiation of ovulation. Estrogen level gradually fluctuates again during postovulatory phase, and then returns to initial level at the end of ovarian cycle. Thus, the rat estrous cycle is used to model the effects of estrogen during the menstrual cycle in women.

Cyclical fluctuation of estrogen level occurs during estrous cycle progression. Estrogen level steadily rises during the diestrus stage and peak during the proestrus stage. Subsequently, estrogen level rapidly drops and then slowly rises to reach a plateau at the estrus stage. From the plateau during the estrus stage, the estrogen level steeply decreases during the metestrus stage and

then increases during the progression towards the diestrus stage. Estrous cycle activity has been implicated as a cause of migraine development because high levels of estrogen during the proestrus and estrus stage can enhance the excitability of neurons in the trigeminal nucleus caudalis (TNC), which results in migraine attacks [6]. Furthermore, estrogen exposure also increases the sensitization of the temporomandibular branch, which is innervated by TG neurons [7]. These results demonstrated that estrogen can affect the trigeminal system.

In the trigeminal nociceptive system, estrogen activates the estrogen receptor (ER) on TG neurons via either genomic or non-genomic pathways. Estrogen modulates neuronal activity through the expression of ion channels or by increasing intracellular cascades, such as extracellular-signal-regulated kinase (ERK) signaling, which phosphorylates various types of ion channels [8, 9]. In addition, previous research has demonstrated that voltage-gated Na channels [10-12] and voltage-gated K channels [13] in dorsal root ganglion (DRG) cells are activated by exogenous estrogen. In other words, activation of voltage-gated ion channels affects AP development in TG neurons, which is a major nociceptive signal from the periphery to higher cortical neurons. Thus, fluctuation of estrogen level during the estrous cycle may alter AP development in TG neurons which correlate to the change of nociceptive inputs from trigeminal system.

Our study aimed to investigate whether the estrous cycle is involved in neuronal excitability of trigeminal system by comparing AP properties of TG neurons in four different stages of estrous cycle. The AP properties reflect the activation of voltage-gated ion channels that affect the excitability of TG neurons. Our results suggested that modulation of the trigeminal system underlies the pathophysiology of menstrual migraine.

Methods

Animals

Female Sprague–Dawley rats, 6-8 weeks old, had a sufficient estrogen level for observing the estrous cycle [14, 15]. Animals used in all experiments were purchased from the National Laboratory Animal Center, Mahidol University, Nakorn-Pathom, Thailand. Rats were housed in stainless cages in a ventilated room under a 12-hour dark-light cycle and were fed ad libitum. All of the protocols were approved by the Animal Care and Use Committee of the Faculty of Medicine, Chulalongkorn University, Thailand (No. 4/58).

Immunoassay of Estrogen levels

Immediately after decapitation, the arterial blood was collected from the left cardiac ventricle for storage in a 1.5-ml microcentrifuge tube. The collection tubes were centrifuged at 3,200 rpm for 10 min. Then, serum was collected and stored at -20 °C. The serum concentration of estradiol (E2) was measured using the Chemiluminescent Microparticle Immunoassay (CMIA) method.

Estimation of estrous cycle stages

Using a dropper, the vagina was flushed by normal saline. Subsequently, one drop of vaginal fluid was placed on a slide and stained with 1% methylene blue. In this manner, vaginal smears were observed under a light microscope (with a 40X objective lens). Four different stages of the estrous cycle were determined by observing

Table 1 RMP and AP properties of TG neurons at each stage of the estrous cycle.#Each variable is shown as the mean ± SEM. *$P <$ 0.05 compared with the diestrus stage (one-way ANOVA followed by *post hoc* test).

Variables	Diestrus (n = 52)	Proestrus (n = 24)	Estrus (n = 35)	Metestrus (n = 27)
RMP (mV)	-46.57 ± 1.13	-47.88 ± 2.38	-49.39 ± 2.46	-41.98 ± 1.86
Threshold (mV)	-19.14 ± 1.76	-27.46 ± 0.52*	-27.00 ± 2.20*	-29.95 ± 3.14
Rheobase (pA)	73.33 ± 3.54	55.63 ± 0.27*	49.58 ± 2.70*	66.36 ± 8.00
AP height (mV)	109.21 ± 3.35	116.66 ± 1.16*	98.24 ± 4.97*	92.53 ± 6.40
AV overshoot (mV)	52.41 ± 2.76	67.41 ± 1.02*	51.63 ± 3.84	39.10 ± 6.56
AP rising time (ms)	1.52 ± 0.63	1.26 ± 0.39	1.24 ± 0.62	1.95 ± 0.93
AP falling time (ms)	5.21 ± 0.40	3.22 ± 0.56*	2.43 ± 0.31*	4.41 ± 0.66
AP duration (ms)	6.46 ± 0.46	4.48 ± 0.20*	3.67 ± 0.31*	5.99 ± 0.82
AHP depth (mV)	-5.10 ±0.49	-12.15 ± 2.36*	-13.56 ± 1.00*	-6.85 ± 1.78
AHP duration (ms)	7.46 ± 1.10	7.92 ± 1.12	5.20 ± 0.82	7.62 ± 2.23

the population of three types of cells in the vaginal smear (i.e., nucleated epithelial cells, cornified epithelial cell and leukocyte, Fig. 2B, 2C and 2D, respectively) [16]. Total 138 female rats were used in the experiment. There were 52 rats in diestrus stage, 24 rats in proestrus stage, 35 rats in estrus stage and 27 rats in metestrus stage (Table 1).

Primary culture of TG neurons

Primary dissociated TG neurons were cultured as described previously [17-19]. Briefly, rats were euthanized with an overdose intra-peritoneal injection of sodium pentobarbital (1 ml/1 rat) before decapitation. Both trigeminal ganglia were removed and placed in a 35-mm culture dish of ice-cold Hank's Balance Salt Solution (HBSS) with penicillin/streptomycin (10-20 µl; 10,000 U penicillin and 10 mg streptomycin/mL), washed twice in HBSS, and sectioned into small pieces with a sterile razor blade in 1 ml of HBSS. Collagenase (100 µl; 2 mg/mL) and dispase (200 µl; 50 U/mL) were filtrated using a 0.22-µm filter and then added to the sample. Immediately following filtration, the sample was incubated at 37 °C for 20 min. Papain was filtered and added, and then the sample was incubated at 37° C for 20 min again. Afterwards, the sample was centrifuged at 1,500 rpm for 2 min, and the supernatant was removed. The precipitate was triturated 3 times in L-15 complete medium using a glass pipette. Next, the sample was centrifuged at 1,500 rpm for 8 min. The precipitate was collected and washed twice with F-12 complete medium. Finally, 400 µl of F-12 complete medium was added to the sample and placed into a 35-mm Laminin/PDL dish for incubation in an incubator (37 °C, 5% CO_2) for 3 hours. The sample was washed twice with F-12 complete medium for further electrophysiological study [20].

Electrophysiological recording

Whole-cell patch clamp recording was used to record the electrophysiological and AP properties of dissociated TG neurons that were maintained in primary culture for 3 hours. Plastic chambers containing trigeminal neurons were placed on the microscope sample stand (Olympus BX51WI microscope, Olympus, USA), after which the cells were superfused with extracellular solution flowing into the plastic chamber at a flow rate of 1 ml/min at room temperature. The extracellular solution was composed of 145 mM NaCl, 5 mM KCl, 2 mM $CaCl_2$, 1 mM $MgCl_2$, 10 mM D-Glucose and 10 mM HEPES; the pH value was adjusted to 7.40 with 1 M NaOH, and the osmolality was adjusted to 320 mOsm/kg with glucose. Glass microelectrodes with an outer diameter of 1.5 mm and an inner diameter of 0.86 mm (Sutter Instruments, Navato, CA, USA) were pulled on a microelectrode puller (Sutter Instrument) and heat polished using a microforge (Narashige, Tokyo, Japan) to a diameter of 1-2 µm.

Next, microelectrodes were filled by an intracellular solution (composed of 140 mM K-gluconate, 1 mM $CaCl_2$, 2 mM $MgCl_2$, 10 mM EGTA, 10 mM HEPES and 10 mM ATP; osmolality adjusted to 280 ± 5 with glucose). Then, microelectrodes were inserted to the headstage of an Axopatch amplifier (Axon, Sunnyvale, CA, USA). In current-clamp recording, to evaluate AP properties in response to the different stages of estrous cycle, the membrane potential was manually held at -60 mV and injected with a current of 10 pA/step with 100 ms duration. The criteria for successful recording were a minimum 10 min recording time, with a stable RMP of more negative than -40 mV; an amplitude of the action potential that was greater than 70 mV; and an input resistance that was higher than 100 mega-ohm. The protocol was adapted from previous reports [21, 22]. The cell diameter was evaluated as the average of the longest and shortest axis in a BX51WI upright microscope (Olympus, Tokyo, Japan). Only cells with diameter < 38 µm were analyzed.

Assessment of the AP properties

The current clamp injected with brief (100 ms) current pulses from a holding potential at -60 mV is shown in Fig. 1A. The threshold (mV) was the lowest membrane potential that yielded the first depolarization phase of an AP. Rheobase (pA) was the minimal current injection that was able to cause the depolarization phase of an AP. The AP height (mV) was measured as the elevation of an AP measured from the holding potential to peak amplitude of the AP. The AP overshoot (mV) was measured as the elevation of an AP measured from 0 mV to peak amplitude of the AP. The rising time (ms) was

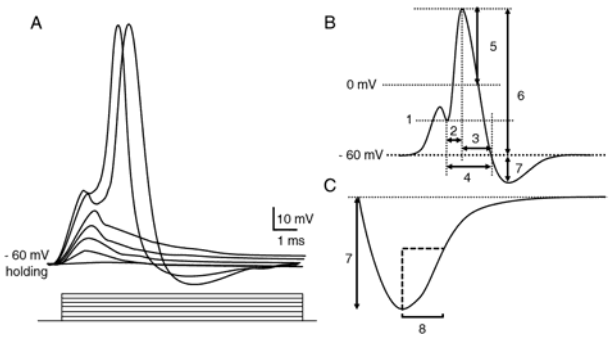

Fig. 1 Assessment of the AP properties. (**A**) Currents in each step are incremented by 10 pA (total 7 currents and 2 spikes). (**B**) 1 = threshold, 2 = AP rising time, 3 = AP falling time, 4 = AP duration, 5 = AP overshoot, 6 = AP height and 7 = AHP depth. (**C**) 7 = AHP depth and 8 = AHP duration

measured as the duration of the rapid depolarization phase, which was measured from the threshold to peak amplitude of an AP. The AP falling time (ms) was measured as the duration of the less positive phase, which was measured from a peak amplitude of an AP to the holding potential (Fig. 1B). The after-hyperpolarization depth (AHP depth mV) is the de-escalation of an AP measured from the holding potential to the negative peak of an AHP. The AHP duration (ms) is the duration time from the negative peak of an AHP to 50% of the recovery of the holding potential (Fig. 1C).

Data analysis

All data are presented as mean ± standard errors of the mean (SEM). Statistical analysis was performed using IBM SPSS Statistics data editor. A one-way ANOVA was used to detect the change among groups that are varied due to the stages of estrous cycle. An independent Bonferroni *post hoc* test was used to determine intergroup differences. A $P < 0.05$ was accepted as statistically significant.

Results

After decapitation, blood serum was immediately collected to analyze the estrogen level. A comparison of the estrogen levels at each stage of the estrous cycle (Fig. 2A) demonstrated that the estrogen level at the proestrus stage (61.00 ± 1.41 pg/ml, $n = 5$) was the highest among the estrous cycle stages (comparing with diestrus, 31.00 ± 2.18 pg/ml, n = 5; *post hoc* test, $P < 0.05$). Furthermore, the estrogen level at the estrus stage was significantly higher than the level at the diestrus stage (46.33 ± 2.89 pg/ml, n = 5; *post hoc* test, $P < 0.05$), whereas the estrogen level at the metestrus stage was significantly lower than the level at the diestrus stage (21.00 ± 2.65 pg/ml, n = 5; post hoc test, $P < 0.05$). The results showed that the overall estrogen level among four different stages of estrous cycle was significantly changed (one-way ANOVA, $P < 0.05$).

The vaginal smear demonstrated that the cytological properties of the vaginal cells changed according to the estrogen level at different stages of the estrous cycle. At the diestrus stage, there were more leukocytes than nucleated epithelial cells (Fig. 2E). In the proestrus stage, there were only clusters of round nucleated epithelial cells, which included a granular cytoplasm and a nucleus (Fig. 2F). In the estrus stage, there were only clusters of cornified epithelial cells (Fig. 2G). In the metestrus stage, there were more leukocytes than cornified epithelial cells (Fig. 2H). However, there were no differences in the morphology of TG neurons at four different stages of

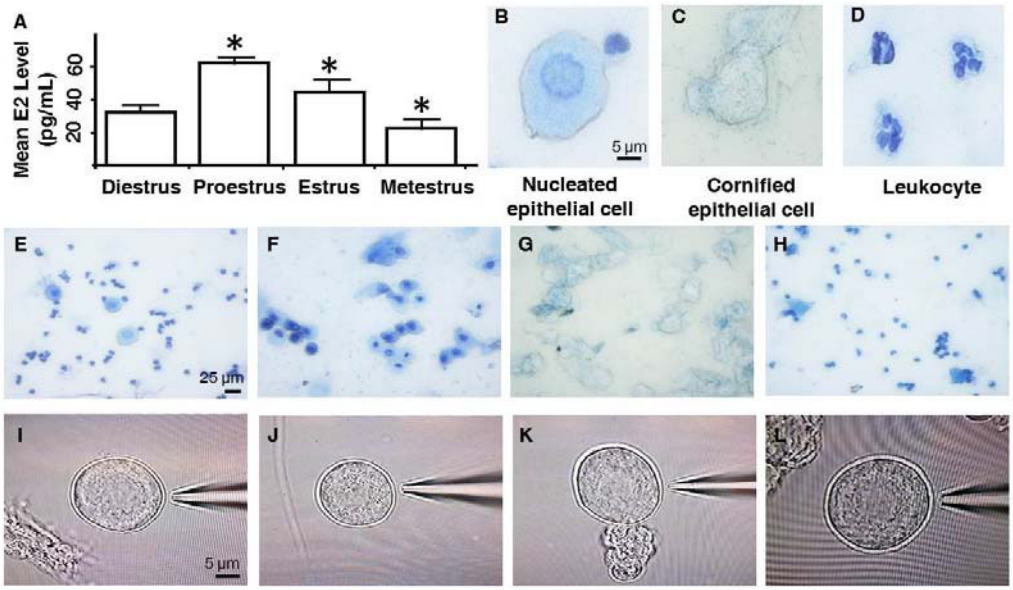

Fig. 2 Evaluation of estrous cycling female rats. (**A**) the concentration of estrogen at each stage of estrous cycle. * $P < 0.05$ compared with diestrus stage (one-way ANOVA followed by *post hoc* test). (**B-D**) representative microphotographs of vaginal cytological samples. (B) Nucleated epithelial cells; (**C**) cornified epithelial cells; and (**D**) leukocytes. Panel (**E-H**), representative samples taken from vaginal smears at each stage of the estrous cycle. (**E**) Diestrus stage, leukocytes appear more than nucleated epithelial cells (**F**) proestrus stage, only nucleated epithelial cells are found; (**G**) estrus stage, only cornified epithelial cells are found; (**H**) metestrus stage, leukocytes appear more than cornified epithelial cells. Panel (**I-L**), representative characterization of primary cultured TG neurons at four different stages of the estrous cycle. (**I**) Diestrus stage; (**J**) proestrus stage; (**K**) estrus stage; and (**L**) metestrus stage. The morphology of TG neurons do not change due to estrogen level or stage of the estrous cycle.

estrous cycle stage (Figs. 2I, 2J, 2K and 2L).

At each stage of the estrous cycle, the dissociated TG neurons in the primary culture were recorded using a whole-cell patch clamp configuration, of which depolarizing current steps were used to stimulate TG neurons to analyze the AP characteristics (Fig. 3A, 3B, 3C and 3D). The TG neurons at each stage of the estrous cycle had similar RMP values (Table 1, RMP, one-way ANOVA, $p = 0.207$). The threshold at the proestrus and estrus stages was significantly lower than thresholds at the diestrus stage (Table 1, Threshold, *post hoc* test, $P < 0.05$, $P < 0.05$, respectively). However, threshold in metestrus stage was invariant to diestrus stage (Table 1, AP threshold, *post hoc* test, $P = 0.422$). The rheobase at the proestrus and estrus stages was also lower than the rheobase at the diestrus stage (Table 1, Rheobase, *post hoc* test, $p < 0.05$, $P < 0.05$, respectively). The AP height and overshoot at the proestrus stage were significantly higher compared to the diestrus stage (Table 1, AP height and AP overshoot, *post hoc* test, $P < 0.05$, $P < 0.05$, respectively). The rising time of the AP was not significant at any stage (Table 1, AP rising time, one-way ANOVA, $P = 0.124$), and the falling time of the AP at the proestrus and estrus stages were significantly shorter compared to the diestrus stage (Table 1, AP falling time, *post hoc* test, $P < 0.05$, $P < 0.05$, respectively). Moreover, the duration of the AP at the proestrus and estrus stage were also significantly shorter compared to the diestrus stage (Table 1, AP duration, *post hoc* test, $P < 0.05$, $P < 0.05$, respectively). The depth of the AHP at the proestrus and estrus stages was significantly deeper compared to the diestrus stage (Table 1, AHP depth, *post hoc* test, $P < 0.05$, $P < 0.05$, respectively), whereas the duration of the AHP was not changed at any stage (Table 1, AHP duration, one-way ANOVA, $P = 0.131$).

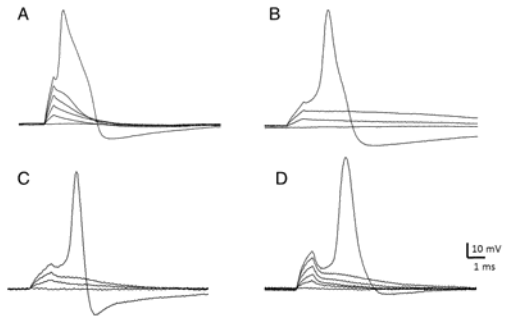

Fig. 3 Representative traces of AP development in TG neurons at each stage of the estrous cycle. (**A**) Diestrus stage (**B**) proestrus stage (**C**) estrus stage; and (**D**) metestrus stage.

Discussion

The present study investigated the effects of four different stages of estrous cycle on the alteration of the AP properties linked to the trigeminal nociceptive system. Each stage of the estrous cycle was associated with differences in the morphology of the vaginal epithelium, which was influenced by the level of estrogen. Our findings are consistent with Goldman, et al. [17]; however, the morphology of the TG neurons did not change, while the properties of the AP were changed.

Estrogen, which binds to ER-alpha and ER-beta receptors, acts via both genomic and non-genomic mechanisms to modulate the pain response, neurotransmitter systems, and other modulatory systems [23, 24]. For AP development in all neurons, voltage-gated Na channels have a key role in response to rapid depolarization, eliciting an AP in TG neurons, which leads to pain perception. Voltage-gated Na channels Nav1.1 to 1.9 are expressed in TG neurons, including Nav1.7 (a tetrodotoxin-sensitive Na channel; TTX-S), Nav1.8 (a tetrodotoxin-resistant Na channel; TTX-R), and Nav1.9 (TTX-R), which can be stimulated to induce an AP [25, 26]. Our results demonstrated that AP threshold, rheobase and AP height were altered in the condition of high estrogen level at proestrus and estrus stages. These findings are consistent with a previous study demonstrating that high estrogen level increases the specific expression of Nav1.8 and Nav1.9, as well as the excitability of trigeminal ganglion neurons by reducing the AP threshold and rheobase and that estrogen also increases the height of the AP [19]. Nav1.7 and Nav1.9 activates at subthreshold resulting to shift of membrane potential closing to AP threshold. After membrane potential reaches AP threshold, opening of Nav1.8 produces AP upstroke in rapid depolarization phase [26, 27]. In addition, estrogen has been shown to increase the expression of ERK [15], which phosphorylates voltage-gated Na channels in TG neurons [28]. Thus, high estrogen level during the proestrus and estrus stages may increase the expression of Nav1.8, Nav1.9, and ERK, which enhances the excitability of TG neurons resulting in lower threshold, lower rheobase and higher AP height of AP development.

Additionally, voltage-gated K channels play a key role during the falling phase, undershoot phase and repolarization phases. Our findings demonstrated that AP falling time were reduced while AHP depth were increased in the condition that estrogen is elevated at proestrus and estrus stages. Previous research has demonstrated that estrogen alters the duration of an AP through the calcium-activated K channel (BK_{Ca}) and changes the depth of AHP through the calcium-activated K channel (SK_{Ca}) in the hippocampal pyramidal neurons [29]. Moreover, estrogen also activates L-type Ca channels to allow Ca^{2+} influx, which increases

intracellular Ca^{2+} and activates voltage-gated K channels [26, 28]. Consequently, a high level of estrogen at the proestrus and estrus stages may potentiate the K efflux during AP development in TG neurons, which presents as shorter AP falling time and deeper AHP depth.

Overall, our results indicated that increase of TG neurons excitability in the condition of high estrogen level during proestrus and estrus stages may involve migraine attacks during menstrual cycle. It has been suggested that activation of voltage-gated ion channels surrounding TG nociceptors induces AP development which increases TG neurons excitability and causes headache pain perception over the migraine attack [30]. Upregulation of voltage-gated ion channels following high level of estrogen may facilitate AP development in TG neurons likely reflects a raise in excitability of the trigeminal system to generate migraine attacks in menstrual migraine, as TG neurons increase their excitability before headache starts. Importantly, the influence of estrogen fluctuation on AP properties changes in TG neuronal excitability may help explain the profound headache observed in menstrual migraine as well as suggest a novel target for the treatment of this migraine condition.

Conclusion

Our study demonstrated that estrous cycle modulates AP properties of TG neurons in intact female rats. Interestingly, modification of AP development in TG neurons at four different stages of the estrous cycle may be induced by the cyclical fluctuation of estrogen levels, which may relate to modulation of voltage-gated ion channels. The results of this study reveal that the neuronal excitability of the trigeminal system increases during menstruation, which may be the fundamental mechanism underlying menstrual migraine.

Acknowledgements The research was supported by the Research Unit and Center of Excellence for Neuroscience of Headache, Integrated Innovation Academic Center, the 2012 Chulalongkorn University Centenary Academic Development Project, the National Research University Project, the Office of Higher Education Commission (WCU-008-HR-57), the Government Research Budget 2014-2019 and the Ratchadapiseksompoj Fund from the Faculty of Medicine, Chulalongkorn University.

Conflict of interest None

References

1. Couturier EG, Bomhof MA, Neven AK, van Duijn NP (2003) Menstrual migraine in a representative Dutch population sample: prevalence, disability and treatment. Cephalalgia 23: 302-308
2. Stovner LJ, Zwart JA, Hagen K, Terwindt GM, Pascual J (2006) Epidemiology of headache in Europe. Eur J Neurol 13: 333-345
3. Dao TT, LeResche L (2000) Gender differences in pain. J Orofac Pain 14:169-184
4. Tassorelli C, Greco R, Allena M, Terreno E, Nappi RE (2012) Transdermal hormonal therapy in perimenstrual migraine: why, when and how? Curr Pain Headache Rep 16: 467-473
5. Staley K, Scharfman H (2005) A woman's prerogative. Nat Neurosci. 8: 697-699
6. Martin VT, Lee J, Behbehani MM (2007) Sensitization of the trigeminal sensory system during different stages of the rat estrous cycle: implications for menstrual migraine. Headache 47: 552-563
7. LeResche L, Mancl L. Sherman JJ, Gandara B, Dworkin SF (2003) Changes in temporomandibular pain and other symptoms across the menstrual cycle. Pain 106: 253-261
8. Amandusson A, Blomqvist A (2013) Estrogenic influences in pain processing. Front Neuroendocrinol 34: 329-349
9. Martin VT, Behbehani M (2006) Ovarian hormones and migraine headache: Understanding mechanisms and pathogenesis - Part I. Headache 46: 3-23
10. Bi RY, Ding Y, Gan YH (2015) A new hypothesis of sex-differences in temporomandibular disorders: estrogen enhances hyperalgesia of inflamed TMJ through modulating voltage-gated sodium channel 1.7 in trigeminal ganglion? Med Hypotheses 84: 100-103
11. Wang Q, Cao J, Hu F, Lu R, Wang J, Ding H, Gao R, Xiao H (2013) Effects of estradiol on voltage-gated sodium channels in mouse dorsal root ganglion neurons. Brain Res 1512: 1-8
12. Hu F, Wang Q, Wang P, Wang W, Qian W, Xiao H, Wang L (2012) 17beta-Estradiol regulates the gene expression of voltage-gated sodium channels: role of estrogen receptor alpha and estrogen receptor beta. Endocrine 41: 274-280
13. Du J, Wang Q, Hu F, Wang J, Ding H, Gao R, Xiao H, Wang L (2014) Effects of estradiol on voltage-gated potassium channels in mouse dorsal root ganglion neurons. J Membr Biol 247: 541-548
14. Norris ML, Adams CE (1979) Exteroceptive factors, sexual maturation and reproduction in the female rat. Lab Anim 13: 283-286
15. Puri V, Puri S, Svojanovsky SR, Mathur S, Macgregor RR, Klein RM, Welch KM, Berman NE (2006) Effects of oestrogen on trigeminal ganglia in culture: implications for hormonal effects on migraine. Cephalalgia 26: 33-42
16. Yener T, Turkkani Tunc A, Aslan H, Aytan H, Cantug Caliskan A (2007) Determination of oestrous cycle of the rats by direct examination: how reliable? Anat Histol Embryol 36: 75-77
17. Malin SA, Davis BM, Molliver DC (2007) Production of dissociated sensory neuron cultures and considerations for their use in studying neuronal function and plasticity. Nature Protocols 2: 152-160
18. Eckert SP, Taddese A, McCleskey EW (1997) Isolation and culture of rat sensory neurons having distinct sensory modalities. J Neurosci Methods 77: 183-190
19. Flake NM, Bonebreak DB, Gold MS (2005) Estrogen and inflammation increase the excitability of rat temporomandibular joint afferent neurons. J Neurophysiol 93: 1585-1597
20. Junsre U, Bongsebandhu-phubhakdi S (2014) ASICs Alteration by pH Change in Trigeminal Ganglion Neurons. J Physiol Biomed Sci 27: 20-25
21. Catacuzzeno L, Fioretti B, Pietrobon D, Franciolini F (2008) The differential expression of low-threshold K (+) currents

generates distinct firing patterns in different subtypes of adult mouse trigeminal ganglion neurones. Journal of Physiology-London 586: 5101-5118
22. Adams JP, Anderson AE, Varga AW, Dineley KT, Cook RG, Pfaffinger PJ, Sweatt JD (2000) The A-type potassium channel Kv4.2 is a substrate for the mitogen-activated protein kinase ERK. Journal of Neurochemistry 75: 2277-2287
23. Martin VT (2009) Ovarian hormones and pain response: a review of clinical and basic science studies. Gend Med 6 Suppl 2: 168-192
24. Fillingim RB, Maixner W (1995) Gender differences in the responses to noxious stimuli. Pain Forum 4: 209-221
25. Dib-Hajj SD, Black JA, Waxman SG (2009) Voltage-gated sodium channels: therapeutic targets for pain. Pain Med 10: 1260-1269
26. Rush AM, Dib-Hajj SD, Liu S, Cummins TR, Black JA, Waxman SG (2006) A single sodium channel mutation produces hyper- or hypoexcitability in different types of neurons. Proc Natl Acad Sci U S A 103: 8245-8450
27. Ostman JA, Nassar MA, Wood JN, Baker MD (2008) GTP up-regulated persistent Na^+ current and enhanced nociceptor excitability require NaV1.9. J Physiol 586: 1077-1087
28. Filardo EJ, Quinn JA, Bland KI, Frackelton AR Jr (2000) Estrogen-induced activation of Erk-1 and Erk-2 requires the G protein-coupled receptor homolog, GPR30, and occurs via trans-activation of the epidermal growth factor receptor through release of HB-EGF. Mol Endocrinol 14: 1649-1660
29. Carrer HF, Araque A, Buno W (2003) Estradiol regulates the slow Ca^{2+}-activated K^+ current in hippocampal pyramidal neurons. J Neurosci 23: 6338-6344
30. Stankewitz A, Aderjan D, Eippert F, May A (2011) Trigeminal nociceptive transmission in migraineurs predicts migraine attacks. J Neurosci 31: 1937-1943